This is the author's version (manuscript) of the work that was accepted for publication in Acta Astronautica
The Version of Record is available online at https://doi.org/10.1016/j.actaastro.20 22.06.029

Terminator Orbits around the Triple Asteroid 2001-SN263 in Application to the Deep Space Mission ASTER

Kai Wickhusen[a,*], Antonio G. V. de Brum[b], Friedrich Damme[c], Alexander Stark[a], Jean-Baptiste Vincent[a], Hauke Hussmann[a], Jürgen Oberst[c]

[a] *German Aerospace Center (DLR), Institute of Planetary Research, Berlin, Germany*
[b] *Federal University of ABC, SBC, São Paulo, Brazil*
[c] *Technical University Berlin, Germany*

Abstract

We search for stable orbits in the vicinity of the triple asteroid system, 2001-SN263, which will be target of the deep space mission ASTER, currently under study by the Brazilian space agency (AEB). Our numerical simulations include gravitational forces caused by the three bodies of 2001-SN263, higher-order terms of the primary's gravity field, planetary perturbations and solar radiation pressure. Due to the low gravity of the triple system, the spacecraft's motion becomes complex and the faint gravity forces of the secondaries are exceeded by radiation pressure from the Sun. However, we show that the so-called "terminator orbits" within the asteroid system at distances between 6-10 km to the primary body can be found. A spacecraft parked in such orbit will stay within the system for several months without the need to adjust its trajectory. Additionally, these stable orbits will allow investigating the entire primary body including its poles as well as the two secondary bodies. We also show that a laser altimeter, which is part of ASTER's primary payload, will benefit significantly from these terminator orbits.

Keywords: Brazilian Space Mission ASTER, ALR – ASTER Laser Rangefinder, Near Earth triple asteroid 2001-SN263, Quasi-Terminator Orbits, Main observational campaign, Numerical integration

1. Introduction

The inner Solar System is populated by a large number of small bodies, the Near-Earth Objects (NEOs), approaching or crossing the orbits of the terrestrial planets. More than 28,000 NEOs have already been discovered and hundreds of new ones are discovered each year [1]. These objects are believed to be remnants from the formation of the Solar System about 4.6 billion years ago. Some NEOs follow trajectories, which cross Earth's orbit – and can possibly collide with our planet. Depending on their size and velocity, such collisions may have dramatic consequences for Earth's ecological system or the human population [2, 3]. It is obvious that our knowledge on the physical properties, the dynamics and evolution of NEOs is critical.
Much knowledge about the structures and dynamics of NEOs can be obtained from multiple NEO systems. A large fraction of the NEOs (15%) are binaries, i.e., systems featuring a primary object orbited by a smaller secondary [4, 5, 6]. While the origins of such binaries are still being discussed, their formation can be explained if the asteroids in question are invoked to have "rubble pile" structures, implying that the asteroids consist of loosely bound material instead of monolithic structures. Small asteroids are observed to undergo a spin-up due to the YORP (YarkovskyO'Keefe-Radzievskii-Paddack) effect [7]. With increasing spin, centrifugal forces may cause a disruption and release of particles that can then re-accrete to form one or several small satellites [8]. Alternatively, satellites may form by single catastrophic disruptions [9] . The YORP-effect in binary systems (termed BYORP) may also modify the asteroids' orbits within the system,

*Kai Wickhusen
Email address: kai.wickhusen@dlr.de (Kai Wickhusen)

leading asteroids to be locked in spin-orbit resonance [10]. Also, tidal effects may be important. Tidal interaction between the primary and secondary may affect the semi-major axes and eccentricities of the orbits resulting in the secondary's escape or tidal decay (e.g.[11]). Tidal disruption during close planetary encounters may support the formation of binaries or multiple asteroid systems [4] – or it may be responsible for disruption of the system. A combination of the YORP or BYORP effects, chaotic orbital evolution and tidal effects can lead to the formation of unique triple systems [9], which may reveal even more information about the formation of multiple NEOs.

The first identified triple asteroid 2001 SN263 was discovered in 2001 and initially classified as a binary system. In 2008 the "Amor-type" object (approaching the Earth's orbit without crossing it) was observed by the planetary radar station of Arecibo, in Puerto Rico, which led to the discovery that 2001 SN263 was in fact a triple system [12]. This was the first triple NEO known at that time. In 2009, a second triple system, 1994 CC, was identified [13]. Furthermore, in 2017 the NEO 3122 Florence was identified as the third triple system, when it had an Earth flyby (see: NASA, JPL Center of Near Earth Object Studies (CNEOS): Radar reveals two moons orbiting asteroid Florence, Sep 1, 2017).

The analysis of the observational data of 2001 SN263 [14, 15] suggested that the primary is approximately a spheroid with an equivalent diameter of about 2.6 km (2.8 × 2.7 × 2.5 km) and smaller companions, about 700 m and 430 m in diameter orbiting at distances of 16.6 and 3.8 km, respectively. Here, we follow the nomenclature adopted by [5], referring to the central (most massive) body as Alpha, to the second most massive body as Beta and to the least massive body as Gamma.

Dynamical solutions for the two triple systems, 2001 SN263 and 1994 CC were presented by [5]. Using numerical integrations of the N-body problem and radar observations as constraints, they derived the masses of the components, the J_2 gravitational harmonic of the central body, and orbital parameters of the satellites (Table 1).

	Alpha (primary)	Gamma (inner)	Beta (outer)
mass, 10^{10} kg	917.466 ± 2.235	9.773 ± 3.273	24.039 ± 7.531
mean diameter, km	2.5 ± 0.3	0.43 ± 0.12	0.77 ± 0.14
mean density, g/cm^3	1.1 ± 0.2	2.3 ± 1.3	1.0 ± 0.4
J_2	0.013 ± 0.008	0.003	0.007
pole orientation (ecliptic):			
ecliptic latitude β, deg	309 ± 15		
ecliptic longitude λ, deg	-80 ± 15		
pole orientation (ICRF/J2000):			
right ascension α, deg	281.97		
declination δ, deg	-58.20		
semi-major axis, km		3.804 ± 0.002	16.633 ± 0.163
inclination, deg		165.045 ± 12.409	157.486 ± 1.819
argument of pericenter, deg		292.435 ± 53.481	131.249 ± 21.918
longitude of asc. node, deg		198.689 ± 61.292	161.144 ± 13.055
mean anomaly, deg		248.816 ± 11.509	212.658 ± 10.691
orbital period, days		0.686 ± 0.00159	6.225 ± 0.0953
rotation period, hours	3.4256 ± 0.0002	16.4000 ± 0.0004	13.4300 ± 0.0001

Table 1: Orbital elements and physical properties for the primary and secondaries for the 2001 SN263 system. Values for the secondaries are given with respect to the primary asteroid Alpha. Mass, mean diameter, and density are taken from [14]. Semi-major axis, eccentricity, inclination, argument of pericenter, longitude of ascending node, and mean anomaly at epoch, are all referred to MJD 54509 in the equatorial J2000 frame. Given errors are 1-σ formal errors. Following [5], we refer to the central (most massive) body as Alpha, to the second most massive body as Beta and to the least massive body as Gamma (regardless of orbit position). Rotation periods are taken from [16]. The J_2 values for Beta and Gamma were derived from their shapes assuming a homogeneous density distribution (see Section 3.2).

The interest in the first identified triple system 2001 SN263 increased significantly when the Brazilian Space Agency (AEB, Agência Espacial Brasileira) announced ASTER, a rendezvous mission to explore this unique target [17, 18]. Besides being Brazilian's first deep space mission it will also be the worldwide first mission to a triple asteroid system [19].

Several Missions to NEA's such as Hayabusa and Hayabusa 2 have be successfully completed in the last years [20, 21]. The OSIRIS-Rex mission has successfully completed its science operation in the vicinity of (101955) Bennu and is currently on its way back to earth [22]. New mission such Dart and Hera are currently developed or are already on the way to their target and will be the first rendezvous missions to a binary system [23].

Hayabusa 1, Hayabusa 2 and Osiris-Rex consisted of remote sensing phase where the asteroids were studied from different hovering and fly-by positions. After studying the asteroids remotely, the spacecrafts left their safe hovering positions and approached the surfaces of their targets for short touch-an-go landing. The spacecrafts collected samples of surface materials and returned or will return these samples back to earth safely [20, 21, 22]. In contrast to these mission and due to the small size of the spacecraft and mission constraints, the science phase of the ASTER mission will consist only of two different remote sensing phases. During the first phase, the spacecraft will be in a hovering position at 50 km from the primary body. The second phase will consist of a terminator orbit phase with a very low demand for maneuvers. A touch down or even are sample return is not foreseen and would exceed the mission requirements.

The motion of the Aster spacecraft will become complex near the small asteroids system 2001 SN263, where the faint gravity forces are possibly exceeded by radiation pressure from the Sun. Additionally, the secondary bodies cause a strong perturbation when the spacecraft gets closer to the system. However, families of orbit-like motion models exist [24], including the well-known "terminator orbits", where particles move in circular or slightly elliptic paths, with the orbit normal vectors in line with the Sun direction [25, 26].The terminator orbits are members among a family of stable motion patterns, the so-called "Quasi-Terminator Orbits" [27, 28]. In 2013 [29] showed that terminator orbits about the asteroid (101955) Bennu are possible and [30] determined the robustness against maneuver errors. Then, in 2019 Osiris-Rex entered a terminator orbit about a NEA for first time and proved that these orbits are not just theoretically feasible [22].

For the ASTER spacecraft, terminator orbits are an optimal solution to investigate the three bodies remotely from a relatively short distance. Additionally, staying in the terminator orbits will require no or very few maneuvers which reduces the demand for operations and propellant.

Several studies on orbits around the asteroid 2001 SN263 have been conducted in the last years. [31] considered in his model perturbations due to the oblateness of the main body, Alpha, the gravity field of the two satellite bodies, the Sun, the Moon, the asteroids Vesta, Pallas and Ceres and all the planets of the solar system, without taking the SRP (solar radiation pressure) into account. Their results show that, when compared to elliptical and equatorial orbits, an internal orbit is the best choice, especially when this orbit is circular and polar (less perturbed). [32, 33] characterized stable regions around the components of this triple system. Through numerical integration they found two stable regions near Alpha and Beta, respectively, and another region, much beyond the satellites. In addition, retrograde orbits - even though not perfect for remote sensing - were found to be stable. Also without considering the SRP, in their works they point out orbits that are approximately polar, circular and internal (region between Gamma and Beta) as favourable for a mission of exploration inside the triple system. The stability of orbits in the 2001 SN263 system has been investigated also using (semi-) analytical theories taking into account perturbations by solar radiation pressure [34, 35, 36]. More recently, [37] conducted a search for less-disturbed orbital regions to place a spacecraft around the system considering gravity forces and solar radiation pressure. Although they have not considered inclined orbits in this research (this subject is indicated for future studies), only planar ones, their results, presented as perturbation maps, show how the SRP dramatically changes the stability regions around the system. They also provide information on the consumption of propellant to keep a spacecraft as close as possible to a Keplerian orbit in those identified orbital regions. [38] used evolutionary algorithms to search for stable orbits in the vicinity of the triple system. The authors solved a restricted four-body problem including the gravity attraction by Alpha, Beta and Gamma as well as the solar radiation pressure. Where applicable, the results of their work could be confirmed by our simulations, but a large range of additional solutions are presented in this paper.

In this study we search for stable orbits within the triple asteroid system 2001 SN263. In particular we investigate the possibility of moving in terminator orbits which are stable over a period of at least one

month. The study focuses particularly on the mission ASTER and takes the requirements and constraints of the mission into account [18, 39].
The paper is organized in 5 sections. In Section 2 we give details on the Aster mission, the triple asteroid system and terminator orbits. Section 3 summarizes the methods which were used to determine stable areas. In Section 4 we show the results, including stable areas with exemplary orbits and in the last Section 5 the implications of the derived results are discussed.

2. The ASTER Mission

The Brazilian space agency plans to launch a small spacecraft called "ASTER" to investigate the triple Asteroid 2001-SN263. The spacecraft will arrive at the asteroid in December 2024 (backup date: September 2027) and start its first science operation phase [19]. During this first phase the Asteroid is observed from a larger distance at 50 km from Alpha. At the end of this phase, the spacecraft performs maneuvers to get into the system and is positioned on a stable orbit within the system, i.e. between the main and the outer body. During this second phase, maneuvers of the spacecraft shall be avoided. This requirement in combinations with the science requirements makes terminator orbits an optimal choice for this second phase.
To move safely within the system, it is critical for the spacecraft to identify and characterize regions of stability and instability (i.e., where collision or escape are imminent). Furthermore, observational and operational strategies to explore all three asteroids critically depend on availability of stable spacecraft orbits (i.e., orbits that do not requiring expensive correction maneuvers).
Besides the technological motivations, the main scientific goal is the unprecedented on-site characterization of this very interesting triple Asteroid. Inside the selected exploration window, a main exploration campaign is being planned to focus the investigations on the biggest asteroid (Alpha). In terms of scientific goals, the investigation will shed light on the formation of this triple system, and each of its main three asteroids will be separately investigated as to dynamic and orbital properties, shape, size, volume, mass distribution, mineral composition, surface topography and texture, gravitational field and rotation speed. The nominal science phase of the ASTER mission is planed to last for 4 month.
Based on current design studies, the spacecraft will have a total launch mass of 150 kg [40]. The main body is a cube with side lengths of 0.5 m each and a total solar cell area of $20m^2$. The spacecraft model, which was used in the simulations is illustrated in Figure 2

2.1. The ASTER Laser Rangefinder

In 2011 a laser altimeter was selected to be part of the primary payload [41]. The instrument was named ALR (ASTER Laser Rangefinder). The altimeter data to be collected by the ALR will be used to determine the morphology of the asteroids (sizes and shapes), essential for precise determination of their masses and densities. The instrument will acquire data for the characterization of the topographic features on the surfaces (craters, boulders, etc.). The topographic profiles to be constructed will be used in the production of digital elevation models of the surfaces with resolutions of about 10 m horizontal, and 10 m (altitude $D < 50$ km) to 1 m ($D \leq 10$ km) vertical, in illuminated and non-illuminated regions. A minimum of 50% coverage of the surface of the main body Alpha, is required for the main exploration campaign, when all attention is going to be focused on this asteroid. The instrument will also support the fine determination of the orbits and the modelling of gravitational parameters. As additional capacities, the instrument is planned to be also applicable in the navigation, supporting spacecraft maneuvers in the proximity phase, and in the calibration of other instruments (imaging camera and infrared spectrometer). A review of the ALR design can be found in [42] containing a more elaborated description of the instrument configuration and the values of key parameters of its operation. To verify the performance in realistic scenarios the simulator software *ALR_Sim* for the environment and operation of the instrument was developed [43, 44]. After a more complete characterization of all three bodies in the system was published [14], the planning of the mission was further enhanced [45, 19]. Modelling of the test trajectories, the joint dynamics and the operation of the instrument was made and integrated in simulator software *ALR_Sim_Tracks* specially created for this purpose.

2.2. Equatorial and polar coverage

A study on possible encounter trajectories for the first part of the science phase has been carried out by [19]. A favourable encounter trajectory at 50 km from the primary body was identified and characterized, together with predictions of the results (coverage) attainable by the ALR along this trajectory. The mentioned predictions show that a minimum of 58% coverage of the surface of Alpha can be achieved with superior quality (better than the minimum expected, in terms of vertical (less than 2 m) and horizontal (about 10 m) resolution, which are controllable through the insertion of a very small inclination in the encounter trajectory of the spacecraft, and through optimization of the laser pulse frequency). Although satisfactory, according to the science goals of the mission, the achieved results also indicate that the attainable coverage will focus mostly on central areas of Alpha (around its equator), leaving the regions around both poles unexplored. Additionally, simulations also show the unavailability of obtaining altimetry data of the poles from different positions inside any encounter trajectory in the scenario of this mission.

To ensure the coverage of the areas around the poles, a second complementary exploration campaign is discussed and proposed in this paper. Once the altimetry data of the poles in this second part of the main campaign is attained and added to the data acquired in the first part (central region), a global model of the asteroid surface could be built with improved quality. This will fulfil the main goal of the ALR with respect to asteroid Alpha in the main campaign.

This paper describes the search conducted to identify internal orbits in the system that would favour the exploration of the poles (from the laser altimeter point of view) and that could accommodate the permanence of a spacecraft with minimum use of station keeping for a short period of time, of at least 1 month.

3. Methods

3.1. Numerical integration

The spacecraft trajectories around the triple asteroid are calculated with a numerical integrator, which solves the equation of motion. Taking into account the relevant forces that are acting on the spacecraft we solve the following general equation [46]:

$$\ddot{\vec{r}} = -\frac{GM_\alpha}{r^3}\vec{r} + \ddot{\vec{r}}_{ht,\alpha} - \frac{GM_\beta}{r_\beta^3}\vec{r}_\beta - \frac{GM_\gamma}{r_\gamma^3}\vec{r}_\gamma + \sum_{sb}\ddot{\vec{r}}_{sb} + \ddot{\vec{r}}_{srp} \tag{1}$$

with $GM_\alpha = 6.12327 \cdot 10^{-7}\text{km}^3/\text{s}^2$ being the standard gravitational parameter of the primary body and $\vec{r}$ and $\ddot{\vec{r}}$ being the spacecraft's position and acceleration, respectively. The reference frame is centered at the center of mass of the primary body.

The main acceleration acting on the spacecraft is caused by the primary body of the asteroid system. The first term of the equation includes the GM-value of the primary body, GM_α as a point mass. The second term of equation 1, $\ddot{\vec{r}}_{ht,\alpha}$, includes the higher order Stokes coefficients of the primary's gravity field. The secondary and tertiary body are represented by the third and forth term of the equation. Both are included as point masses with their corresponding GM values, GM_α and GM_β. Additionally the large Solar System bodies, such as Sun and Jupiter are also include as perturbing forces in $\ddot{\vec{r}}_{sb}$. The last term takes into account the solar radiation pressure acting on the spacecraft. This acceleration is extremely important in the low-gravity environment of small asteroids.

The acceleration $\ddot{\vec{r}}_{sb}$ caused by solar radiation pressure for a plane surface reflecting one fraction and absorbing the other fraction of the incoming light is given by [46]:

$$\ddot{\vec{r}}_{sb} = -\nu P_{ref}\left(\frac{1AU}{d_{sun}}\right)\frac{S}{m_{sat}}cos\theta[(1-\epsilon)\vec{e}_{sun} + 2\epsilon cos(\theta)\vec{n}] \tag{2}$$

where ν is the shadow function ($\nu = 0$: umbra, $\nu = 1$: sunlight, $0 < \nu < 1$: penumbra). $P_{ref} = 4.56 * 10^{-6}Nm^2$ is the solar radiation pressure at 1 AU, d_{sun} the distance from the surface to the sun, S the surface area, m_{sat} the space probe's mass, θ the illumination angle, ϵ the reflectivity of the surface, $\vec{e}_{sun}$ sun the direction to the sun, and $\vec{n}$ the surface normal. $\nu = 1 - A/(\pi a^2)$ has to be calculated for the given

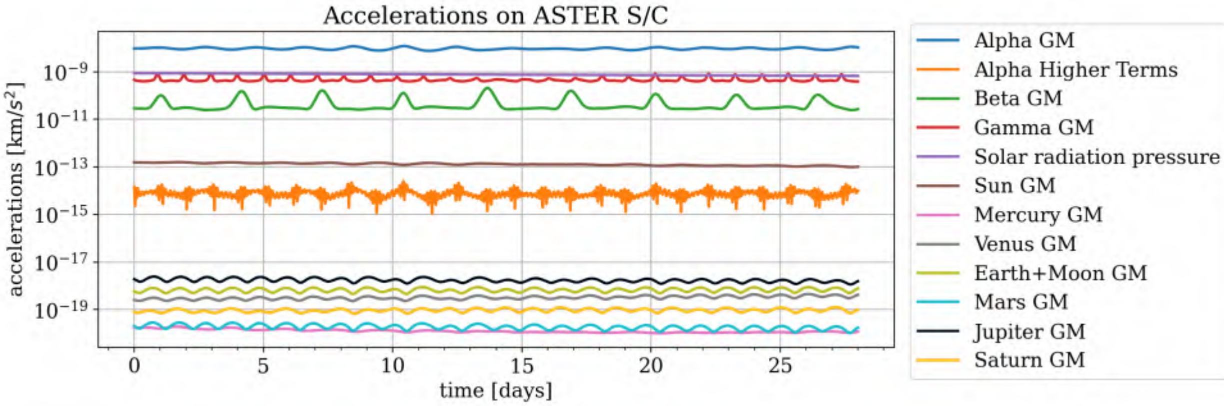

Figure 1: Accelerations acting on the S/C in the reference orbit (at 8 km initial distance from primary, heavy s/c, see 3.1)

spacecraft position and constellation of celestial bodies considered. A is the occulted segment of the sun and a the apparent diameter of the sun. The constellation of bodies is calculated using SPICE routines at the given epoch. The solar radiation pressure, which has to be computed for every time-step depends on the absolute distance to the sun and on the mass-to-area ratio of the spacecraft.
In our simulation the so called box-wing model for S/C geometry was used. It is composed of a cubic shaped with 6 surface areas and two solar panel areas which are orientated perpendicular towards the solar radiation. The bottom surface of the spacecraft's main body cube is always nadir pointing. The spacecraft model is shown in Figure 2 . Based on the information provided spacecraft reference design document [40] the surface areas are defined as:

- 6x 0.25 m^2 (with a reflectivity value of 0.8)
- 2x 10 m^2 (with a reflectivity value of 0.058 or 0.21)

For the simulation two spacecraft scenarios were defined. In the first scenario a S/C with a mass of 150 kg, i.e. with full tank and low reflectivity of 0.058 for the solar radiation pressure was used (**heavy S/C**). In this scenario the solar radiation pressure has a lower effect as in the the second scenario, where the Xenon tank are empty and and the total mass is reduced to 80 kg (**light S/C**). Additionally we assumed a solar panel with less efficiency and a higher reflectivity of 0.21, leading to a higher force caused by SRP.

In summary, the following accelerations were used as force or perturbing force in our model:

- GM of the primary body of the Asteroid (Alpha)
- higher terms of the gravity field of the primary body up to degree and order 20
- GM's of the secondary and tertiary body (Beta and Gamma)
- GM's of solar system bodies (Sun, Mercury, Venus, Earth+Moon Barycenter, Mars, Jupiter, Saturn)
- Solar radiation pressure (one heavy S/C scenario and one light S/C scenario)

All modeled accelerations acting on the S/C in an 8 km reference orbit are shown in Figure 1. It shows that the higher terms of the primaries gravity field as well as the planets of the solar system have only a very small effect and can be neglected. The same applies on accelerations caused by Beta's and Gamma's higher terms gravity field.

It is well know that the stability of spacecraft orbits in the environment of low-gravity NEO's depend on the direction of the incoming solar radiation pressure [25]. Stable orbits are found when their orbital plane

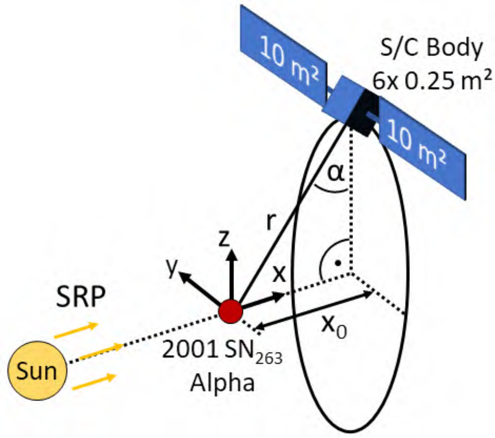

Figure 2: Illustration of the sun oriented co-rotating reference frame and the spacecraft model used in the simulation. The spacecraft is positioned on a displaced terminator orbit in anti-sun or x direction. The spacecraft model consist of a solar panel area of 20 m^2 which is always oriented towards the sun. The bottom side of the spacecraft main body is always nadir pointing. The x-axis of the reference frame is always parallel to the incoming solar radiation and the z-axis perpendicular to the heliocentric orbital plane of 2001SN263.

is chosen to be perpendicular to the incoming radiation. However, to assess the gravitational effects of the secondaries we ran a full scan over the three orbital elements which define mainly the position of the orbital plane relative to the primary body. The following orbital elements were varied:

- a: semi-major axis, range: [2 km - 15 km]
- i: inclination , range [0° - 90°]
- Ω: longitude of ascending node, range [0° - 180°]

3.2. Shape and gravity fields

The gravitational field of all three bodies of 2001 SN263 was modeled in two steps. First, a polyhedral approach was used to integrate the gravitational acceleration contributed by the mass distribution inside the object. Afterwards a volume discretization from [47] was used to integrate over volume elements where each polyhedron is defined by a triangular facets of the shape model, and the center of the shape. This integration is equivalent to the classical approach of [48] for shapes with more than 10 000 facets, but faster to compute. We considered each object to be homogeneous, with the density of each volume element being equal to the bulk density of the asteroid (i.e. $\rho_\alpha = 1100$ kg/m^3, $\rho_\beta = 1000$ kg/m^3, $\rho_\gamma = 2300$ kg/m^3). Although fast, this method requires an integration over each facet for every calculation, and is not suited for long term orbital calculation. We run this analysis once to get a reference gravitational field, calculated on the circumscribing sphere for each object.

In a second step, this reference field was replaced with a spherical harmonics approximation. This is done with the python library SHTOOLS [49] which provides a well tested implementation of this conversion. In short, the gravitational field calculated in the first step from the irregularly sampled shape is expanded into spherical harmonics using a least-squares inversion (function: `pyshtools.expand.SHExpandLSQ`).

As a test, the gravitational acceleration on the reference interface was recalculated from this spherical harmonics expansion and compared it to the polyhedral model from step 1. It showed that using a maximum degree/order of 20 is sufficient for an accurate description of the gravitation field. The mean residual difference between the spherical harmonics approximation of the gravitational acceleration and the value determined by the polyhedral integration is equal to 0.002 %, with a standard deviation of 0.48 %. When applying the same approach to the gravitational potential, the spherical coefficient C_{20} gives us the oblateness factor J_2. We find $J_{2,\alpha} = 0.015$, which is within the range proposed by [14]. Using the same approach

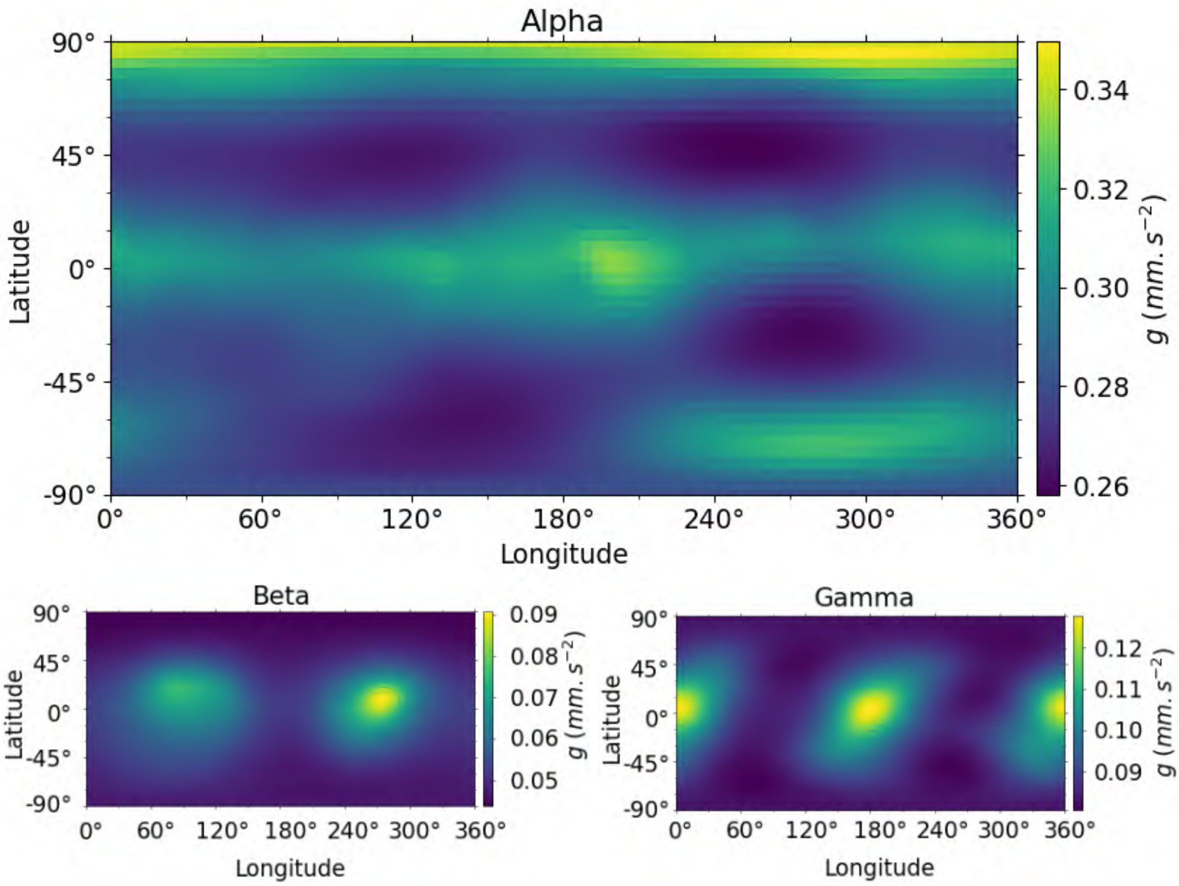

Figure 3: Gravitational acceleration calculated on a sphere circumscribing each asteroid. This field is approximated with spherical harmonics and expanded to further distances.

$J_{2,\beta} = 0.007$ and $J_{2,\gamma} = 0.003$ were determined. With the resulting gravity field coefficients, we are able to determine the acceleration caused by this field. The results are summarized in Figure 3

3.3. Track simulation of the ASTER Laser Ranger

The study aims to identify orbits sufficiently stable for a period of approximately 1 month to allow optimal laser operation from an almost constant distance with the possibility to cover at least 50% of the surface of the asteroid and to scan to pole areas with a laser altimeter. The expected results for the research campaign, in terms covered area with laser altimetry shots, footprints sizes and spacing between successive footprints are provided. The analysis consists of two main steps. The first step involves the search for stable orbits which allow laser ranging from an almost constant distance. This can be satisfied with a terminator orbit. For the second step a simulator software, called *ALR_Sim_Tracks* was developed [19]. This software allows a deeper understanding of the details of the instrument operation and facilitating the definition of parameters during the design phase. The simulation procedure carried out with use of this tool is described in the following.

i) Trajectories and orbits: for the simulations, spacecraft and asteroid orbits were generated for the period from 12h of 07/Feb/2025 to 12h of 07/March/2025 (Ephemeris Time - ET, 60 sec spaced data), in the Sun centred ecliptic J2000 frame.

The position and velocity vectors of asteroid Alpha are given by $\vec{R}_{ast}(t) = (X_{ast}, Y_{ast}, Z_{ast})$, and $\vec{V}_{ast}(t) = (VX_{ast}, VY_{ast}, VZ_{ast})$. The position and velocity vectors of the ASTER spacecraft when it follows the reference orbit are denoted by $\vec{R}_{sc}(t) = (X_{sc}, Y_{sc}, Z_{sc})$, and $\vec{V}_{sc}(t) = (VX_{sc}, VY_{sc}, VZ_{sc})$. The program will accept any trajectory as input data. In this scenario, the 8 km reference orbit (see Figure 8) was given as input data.

ii) Modelling of asteroid Alpha's physical and dynamic features [14]: 2001SN263 Alpha is modelled as a ellipsoid with the following main axes: $(d_x, d_y, d_z) = (2.5, 2.4, 2.1)$ km). Its rotation period is set to 3.4 hours and the pole direction (ecliptic longitude and latitude): $(\lambda, \beta) = (309, -80) \pm 15$ deg (see also Table 1.)

iii) Laser altimeter simulation: When the spacecraft is in a terminator orbit around asteroid Alpha, the nadir pointing condition is used as reference case, i.e. the instrument line of sight points towards the body's center of mass. For each emitted laser pulse (modelled as a line pointing from the spacecraft in the direction of the asteroid's center of mass) the intersection with the asteroid's surface is calculated. The determined intersection point is identified and the footprint size is calculated. The list of all footprints is stored for later analysis.

The following instrument parameters were assumed:

- **Divergence angle (θ_{div})**: this parameter directly affects the footprint size. The planned size of the footprint is 5 to 10 m (radius), at 10 km. To have such footprints, values from 500 μrad to 650 μrad (half cone) are considered for this angle.

- **Pulse repetition frequency (PRF)**: this parameter directly affects the spacing between successive footprints in a surface scan, named along-track distance (ATD), consequently affecting the quality of the surface mapping in terms of horizontal resolution.

From the ALR preliminary design, the reference PRF value is 1 Hz and, associated to this operation rate, the data generation rate is 12 bytes/sec [41, 42]. However, previous results of this research pointed to the possibility of using smaller PRF values (e.g. 1/20 Hz) as sufficient to get the desired coverage. Nevertheless, 1 Hz was chosen as PRF in the simulation. The LIDAR instrument on board mission Hayabusa-2 mission also had a maximum PRF of 1 Hz [50] and can was considered as reference case.

With these inputs, the scanning of the asteroid surface by the laser altimeter is simulated for the complete time frame. The list of all points of intersection, called footprint centres, is generated. From the analysis of this list and associated data the results of the simulated exploration campaign are extracted. Each footprint has its position, distance, minimum radius and minimum covered area calculated. The analysis of the distribution of points and covered areas over the target surface allows to predict the type of coverage (qualitative and quantitative) that will be obtained for the inputs used.

4. Results

Our analytical evaluation and our numerical calculation show that stable orbits can be found in the vicinity of the triple asteroid. Especially at distance between 6 to 10 km from the primary, large stable areas have been identified. With a semi-major axis of approximately 8 km +-2 km, the optimal solution are between the orbits of the the secondary and the tertiary body. These orbits could be of high scientific interest for studying this complex 3-body asteroid.

4.1. Analytical predictions

Due to the numerous perturbing forces acting on the S/C numeric integration is necessary for orbit simulation. But analytical predictions can help limiting the regions where stable or even frozen orbits may occur.

Perfectly circular terminator orbits occur only in a very reduced model: the two-body problem plus a constant pressure force originating form a unmoving sun. An orbit with constant distance r to the asteroid must have an orbital plane displaced behind the asteroid (see Figure 2). The displacement x in anti-sun direction is given by [27]:

$$x = \frac{a_{srp}}{GM} r^3 . \quad (3)$$

With a_{srp} denoting the acceleration caused by the pressure force and GM central force of asteroid mass M. If distance r is big the orbit becomes unbound. Linear stability can be inspected by introducing small initial perturbations $x + \delta x$ and $r + \delta r$ to the orbit solution [27]. As result we get a limit on the distance r of a stable circular terminator orbit:

$$r \quad < \quad \sqrt{\frac{GM}{3a_{srp}}} \tag{4}$$

This is a easy to use criteria for terminator orbit size, but only valid for time intervals where the asteroids movement about the sun can be neglected.
To study longtime effects The Augmented Hill Three-Body Problem introduces the eccentric orbit of the asteroid around the sun. Orbit approximations found by averaging the effects of solar radiation pressure over one orbit of the S/C, were always stable and periodic [25]. Also the S/C orbit liberates around a sun-synchronous state, e.g. a terminator orbit will rotate the orbit normal to follow the sun. The eccentricity changes periodically with the same period T as the liberation of the orbit plane.
Unstable orbits will only occur if the eccentricity is too high and the S/C is to close to the surface or the averaging method is not applicable. Small orbits become more eccentric and we get a lower bound for orbit size. The eccentricity of a frozen terminator orbit (no liberation) described in [25] was used to find the lower bound in Figure 4 to avoid hard landing. Large S/C orbits have a higher period P for one revolution over which we averaged. Is $P \geq T$ the method is invalid. Sun-synchronous orbits of this size are necessarily unstable and were blown away by SRP in numeric simulations. Through numeric experiments we are sufficiently confident in the averaging method as long as:

$$4.1 \cdot P \quad < \quad T \tag{5}$$

In Figure 4 this criteria in used to give a maximum semi-mayor axis for stable sun-synchronous orbits.

4.2. Frozen terminator orbits

For carefully chosen initial states the orbit does not liberates around a sun-synchronous state. In the co-rotating frame of the asteroid this orbit is 'frozen'. Due to interactions with the asteroids shadow we do not consider the frozen orbits with $i = 0°$. Again, by averaging the effects of solar radiation pressure over one orbit of the S/C, the works of [25] give us the constant orbital elements of a frozen orbit:

$$\begin{aligned} i = \quad \Omega = & \quad \pm 90° \\ \omega = & \quad \mp 90° \\ e = & \quad \cos\psi \end{aligned} \tag{6}$$

With the constant ψ defined by the relation of asteroid gravity, centripetal force and SRP:

$$\tan\psi \quad := \quad \frac{3a_{srp}}{2\nu'_{\text{hel}}}\sqrt{\frac{a}{GM}} \tag{7}$$

If SRP is weak, then $\psi \to 0$ and if SRP is strong relative to gravitational forces, then $\psi \to 90°$. ψ is constant because solar distance is canceled out from $a_{srp}/\nu'_{\text{hel}}$ in Eq. (7).
It is important to remember that the solutions for a, e, i, ω and Ω in Eq. (6) are averages over one orbit and are referring to the co-rotating frame. Frozen and other terminator orbits still have a displacement x in anti-sun direction, positioning the orbital plane behind the small body. Even if the average inclination i is frozen at 90° the actual inclination must differ to account for the displacement x. For a frozen terminator orbit the optimal initial offset is [51]:

$$x_0 \quad = \quad \frac{a_{srp}}{GM}\; a^3\; (1-e)(1+\frac{e}{4}) \quad \text{if } \nu_0 = 0 \tag{8}$$

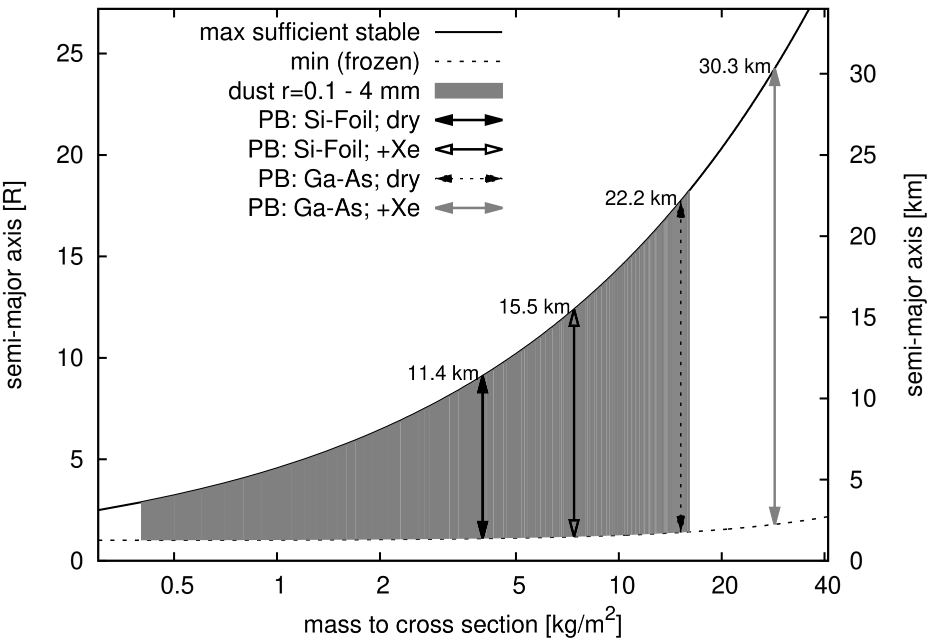

Figure 4: Semi-mayor axis (in km or primary asteroid radius R) of stable and periodic orbits depending on orbiter mass to cross section. The area between the upper and the lower curve is the region were stable terminator orbits can be found. Reference values are given for different ASTER case models and grains of dust; ASTER dry mass 80 kg; xenon (Xe) capacity is 70 kg; effected area with Si-foil photoelectric battery: $20.25m^2$, with Ga-As photoelectric battery: $5.25m^2$; total reflectively of S/C and dust is 0.093 (0.8 ASTER main body, 0.058 Ga-As panel, 0.0844 Si-foil); dust is assumed to be spherical; secondary bodies of 2001Sn263 are not considered

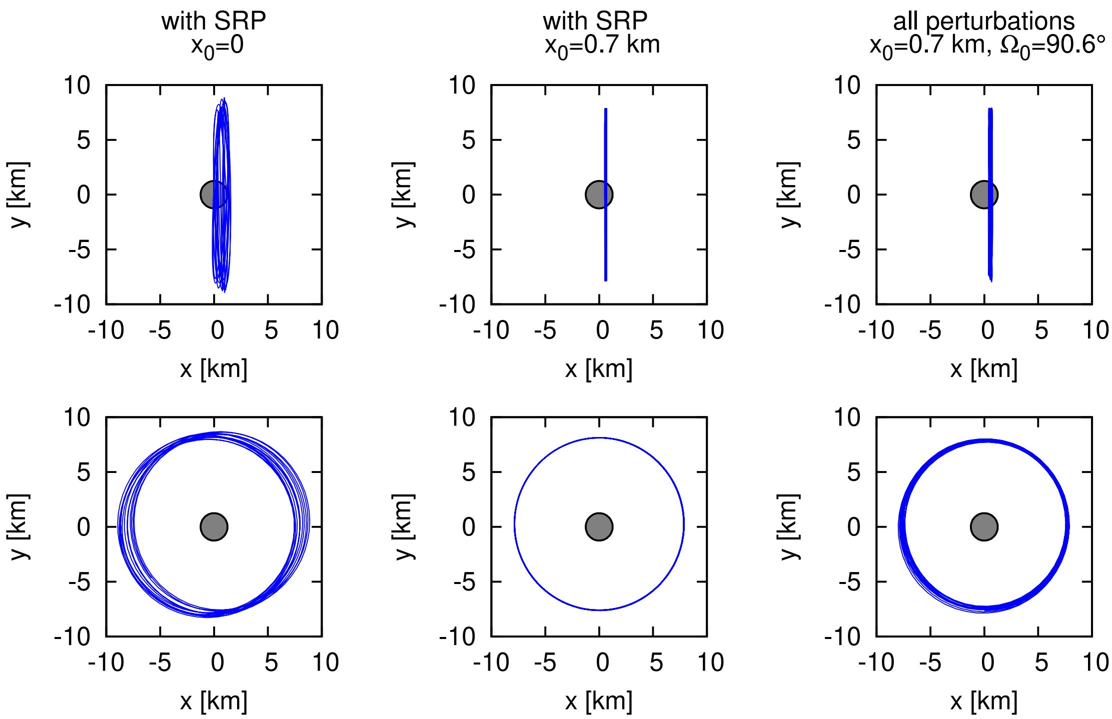

Figure 5: Numeric simulation for light s/c (80 kg, refelctivity = 0.21), see also 3.1. Frame is co-rotating with Sun-asteroid line x, z orientated along the asteroid's orbit normal and y orthogonal to x and z. Initial state: $i = 90°$, $\Omega = 90°$, $\omega = -90°$ and anomaly $\nu = 0°$. Over the 30 days of integration solar distance rises from $1.27AU$ to $1.44AU$. **Left:** Frozen eccentricity $e = 0.0325$ chosen according to Eq. 6. **Middle:** Augmented frozen eccentricity $e = 0.0323$ and shift of orbit in anti-sun direction x_0 chosen according to [51] algorithm 2. **Right:** all perturbations are included in simulation, in particular moonlet gravity. Elements $e = 0.091$ and $\Omega_0 = 90.6°$ adapted to compensate for moonlet gravity.

This offset is consistent with the result Eq. (3) in the static 2-body problem. x_0 has the factor a_{srp} and therefore is anti-proportional to the square of the changing solar distance. Our numerical simulations, in Figure 5, show that the displacement x will adapt to this changes consistent with Eq. (8), keeping the other elements frozen.

In an algorithm in [51] the frozen eccentricity was improved by using an 'effective' semi-major axis $a' = a(1 + a^4 a_{srp}^2/GM^2)^{3/2}$ to calculate frozen eccentricity e using Eq. (6, 7). The 'effective' semi-major axis is defined to be consistent with the velocity $\dot{r}$ of the displaced orbit.

Perturbing effects from the J2 and J3 term of the asteroid gravity on the frozen state (Figure 5) were too small in the simulation to be noticeable. Therefore we did not apply the corrections to the inclination and eccentricity to compensate for the J2 and J3 term proposed in [51]. But eccentricity and ascending node Ω were mortified in the simulation in Figure 5 to compensate for moonlet gravity. Frozen terminator orbits are strictly periodic therefore particularly robust to initial state and dynamics perturbations in the numerical experiments of [52].

4.3. Orbital stability

The orbit stability is defined as (dist$_{max}$ - dist$_{min}$) / dist$_{init}$ to the primary body, i.e. maximal distance over one month - mininal distance over one month divided by the initial distance. This criteria is comparable to the keplerian eccentricity, i.e. if the eccentricity stays below a certain value, the orbit would also be considered as stable. However in the vicinity of the such a triple asteroid where the secondary and tertiary

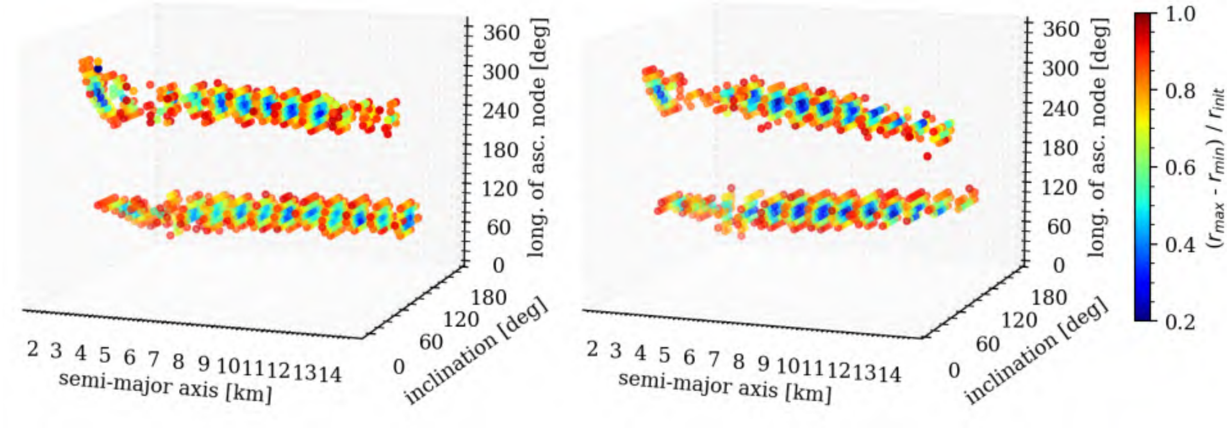

Figure 6: Stability results for initial distances between 2 km to 14 km from the primary body. **Left**: heavy s/c (150 kg, reflectivity = 0.058), **Right**: light s/c (80 kg, reflectivity = 0.21), see also 3.1. Each point of the Figure represents an orbit which is stable over 30 days. Reference Frame: ICRF/J2000. The stability is defined by maximal distance to primary over 30 days minus minimal distance divided by initial distance. A detailed overview of the planes at semi-major axis = 6, 8 and 10 is found in Figure 7

bodies play an important role and the solar radiation pressure is one of the strongest forces acting on the space, a nominal eccentricity is hard to determine. Thus, we used and absolute distance criteria. Additionally, minimizing the eccentricity and consequently the absolute distance variation, will give better results for the laser altimeter. In Figures 6 and 7 a hypothetical value of 0 would lead to a spacecraft orbiting the primary body in a perfect circle. Of course, this is an unrealistic scenario and is not obsevered in our simulation, but in the best cases we obtain a value of less than 0.2. In this case, at an exemplary initial distance of 8 km, the spacecraft would mainly stay at this distance and have a variation better than ± 0.8 km in total. In other words, in this case the orbital distance would vary between 7.2 km and 8.8 km.

The numerical simulations suggest the existence of optimal stable regions in distances of about 6 to 10 km from the primary body. In Figure 6 the results of the simulations are shown. In these areas, the spacecraft may stay in a stable orbit for at least one month with no or very little need of additional station keeping maneuvers. Our simulation show that both cases with strong (light spacecraft) and low (heavy spacecraft, see Section 3.1) accelerations caused by solar radiation pressure will allow finding stable regions but located differently in the three dimensional space (inclination, longitude of ascending node and semi-major axis). In both cases an initial distance of 8 km to the primary will allow getting in to a stable orbit.

4.4. Results of the laser tracks simulator software

The predicted exploration results for the second part of the main campaign and the implication on the laser ranging are presented in this subsection. This second part, consisting of the terminator orbit phase, is used to simulate the laser altimeter tracks and simulate its coverage. For this purpose, the reference terminator orbit at 8 km distance from the primary was used (see Figure 8). The following setting were applied for the simulation:

- Epoch: 07/Feb/2025 to 07/March/2025 (60 sec spaced data).
- Instrument: divergence angle (θ_{div}; half cone) = 650 μrad; PRF = 1 Hz.
- Spacecraft: nadir pointing (instrument points to Alpha's center of mass).

Figure 8 shows the ASTER spacecraft in its reference orbit within in the triple Asteroid system at 8 km difference from the primary body during the exploration period considered in this simulation. It shows that the s/c completes only 13 orbits around the main body during this period. For a fixed period of investigation, this reduced number cannot be raised because it depends only on the chosen reference orbit. In this case, the coverage attainable depends on the chosen distance and on the asteroid dynamics. To improve the coverage from the 13 orbits depicted in Figure 8, the quality of the altimetry data to be collected by the

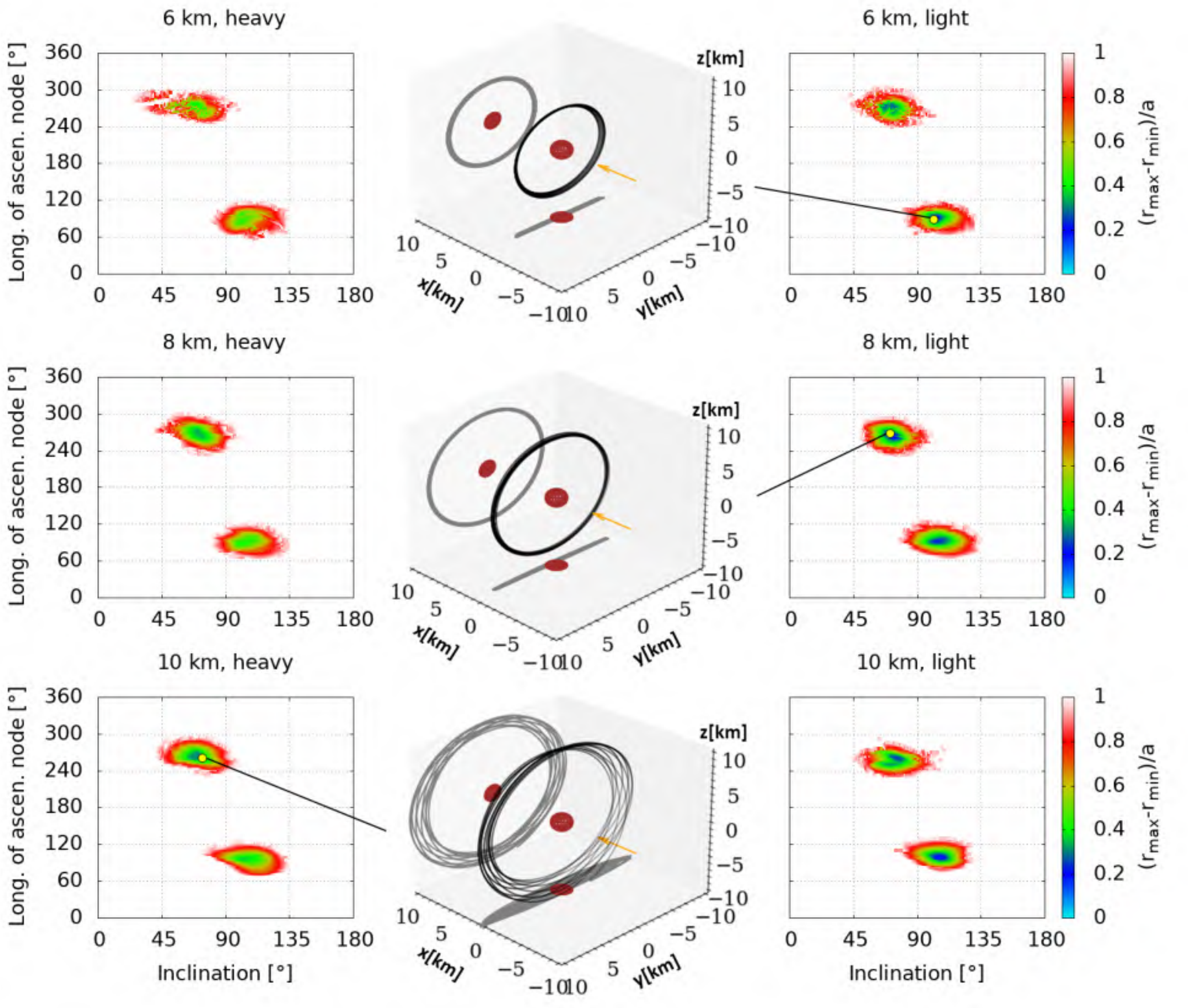

Figure 7: Detailed stability results for initial distances at 6, 8 and 10 km. See also Figure 6. **Left**: heavy s/c (150 kg, reflectivity = 0.058), **Right**: light s/c (80 kg, reflectivity = 0.21), see also 3.1. Each point of the Figure represents an orbit which is stable over 30 days. Reference Frame: ICRF/J2000, reference plane: earth mean equator. The stability is defined by maximal distance to primary over 30 days minus minimal distance divided by initial distance. **Middle**: Three exemplary orbits for 6, 8 and 10 km initial distance. Frame is co-rotating with Sun-asteroid line x, z orientated along the asteroid's orbit normal and y orthogonal to x and z. The orange arrow represents the incoming radiation. Each orbit is referenced to the corresponding points in the color coded map. Each three dimensional orbit and the primary body are projected to the xy- and yz-plane for a better visualisation. The orbits of the secondary bodies are not shown, although they were included in the simulations. A detailed view of the 8 km orbit including the orbits of the secondaries is shown in Figure 8

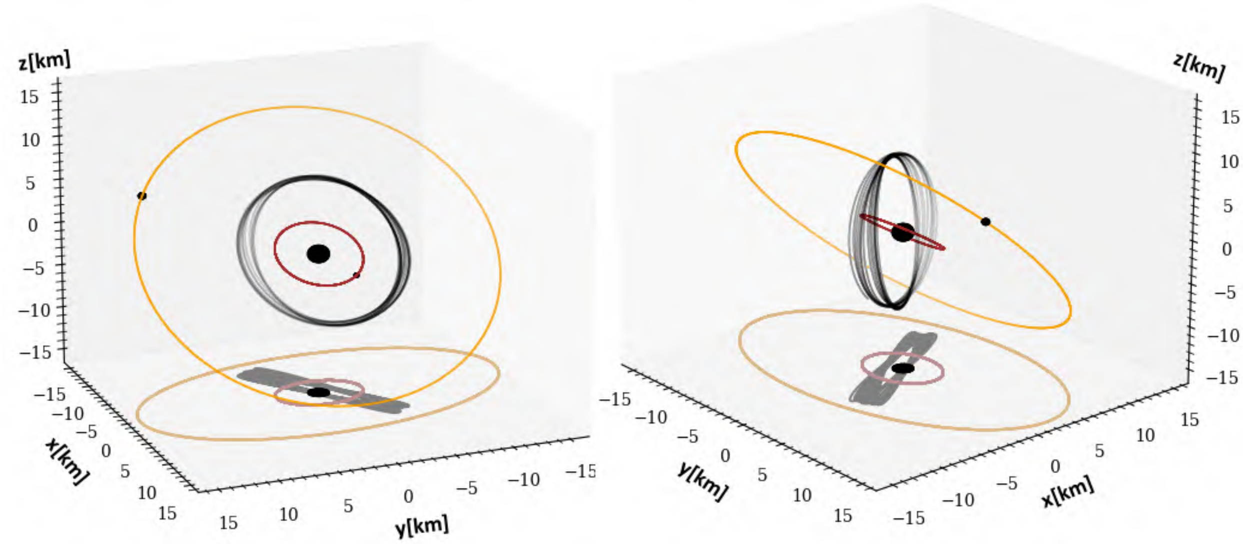

Figure 8: Two different perspectives of the ASTER spacecraft in its reference orbit within in the triple Asteroid system at 8 km difference from the primary body (black line). The time frame is 1 month. This orbit is identical to the 8km orbit shown in Figure 7. Orbits of the secondary bodies (red and orange) and their starting position at epoch 07/Feb 12:00 are also shown. Body size and orbtial radii are in correct scale. For a better visualisation, the orbits are also projected to the xy-plane. Reference Frame: Heliocentric Ecliptic J2000 frame.

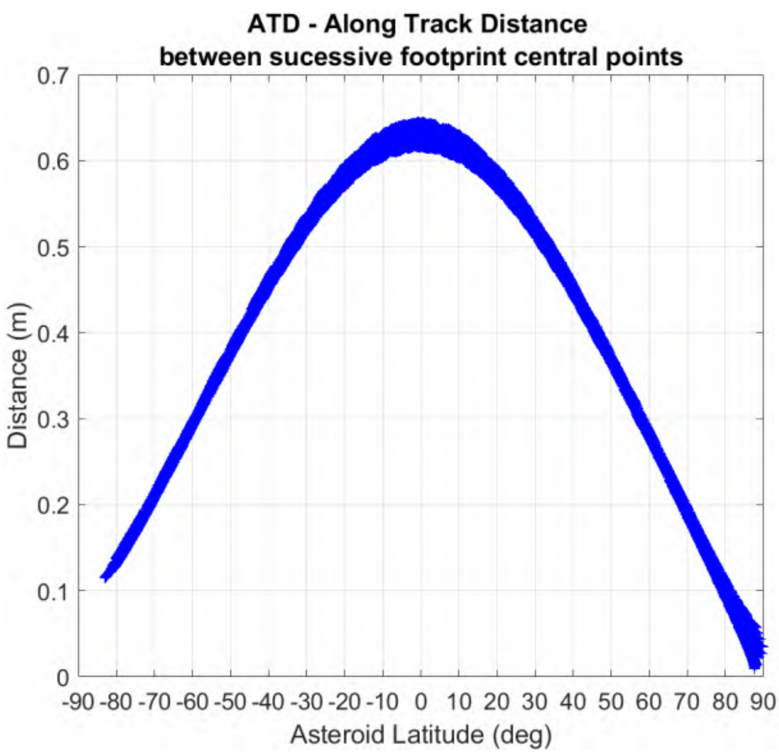

Figure 9: ATD for the simulated reference T.O. when PRF=1 Hz and θ_{div}=650 μrad. The calculated footprint diameter in this case measures 9.0±1.5 m. ATD values directly influence the horizontal resolution.

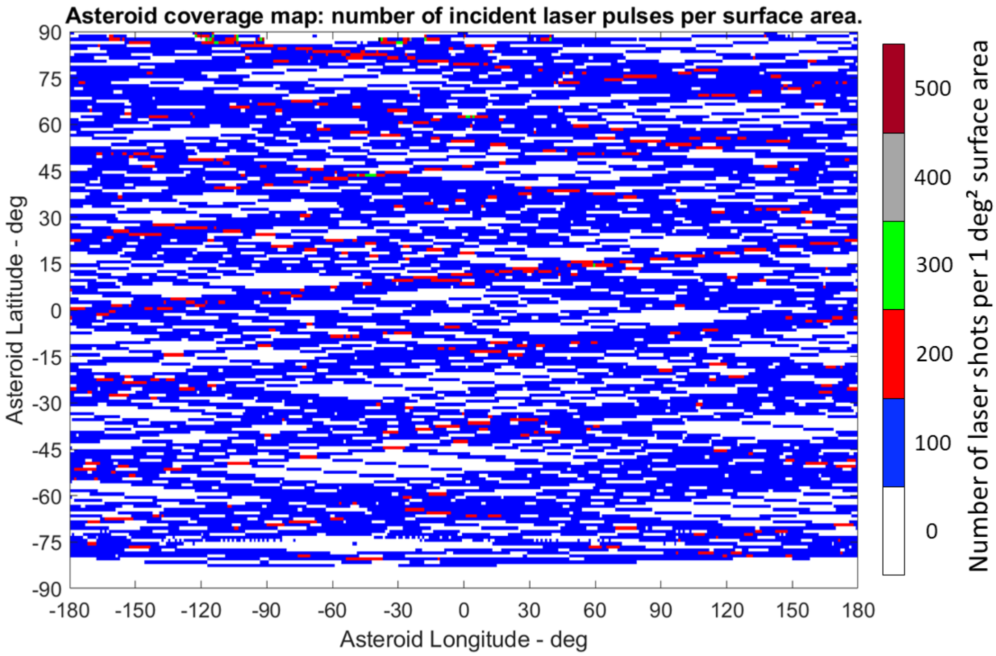

Figure 10: The coverage attained is presented through a flat latitude-longitude map of the density of altimetry measurements per area of 1x1 degrees on the surface of asteroid Alpha. Parameters are: PRF=1Hz, θ_{div}=650 μrad.

laser altimeter must be raised. To do that, a high PRF is indicated. In this case, 1 HZ means an ATD (Along Track Distance) smaller than 1 m (0.1 - 0.7 m) for footprint diameters of about 8.9 m. The coverage of the surface is simulated by splitting the surface area in 180x360 deg^2 elements. Afterwards each surface element is evaluated and the number of laser shots within this element is counted. The coverage of the surface of Alpha attained in the whole complementary exploration campaign is represented in Figure 10 in terms of a flat latitude-longitude map with the number of altimeter measurements per area. This Figure shows a remaining uncovered cap around the south pole. In this simulated case, the central values assumed for the spin axis of Alpha (ecliptic longitude and latitude) are (λ, β)=(309, -80) (see Table 1). In fact, because of the large uncertainty in the current knowledge about the direction of the spin axis (±15 deg [14]), one cannot guarantee a perfect coverage of both poles. However, inside this uncertainty margin, it is possible to achieve a better situation regarding the complete coverage of the poles. Nevertheless, unless the mentioned uncertainty is reduced, there is no how to guarantee the desired coverage will actually occur. Because of this fact, the availability of an "off-nadir" attitude mode is recommended for this mission.

5. Discussion and conclusions

In this paper we have confirmed that stable terminator orbits exist about Asteroid 2001 SN263. In application to the ASTER mission we found several optimal terminator orbits which fulfill the requirements in terms of coverage and stability. Additionally, we showed that the gravity fields of Beta and Gamma have only a negligible effect on stability while the higher terms of the primary body's gravity field play an important role.

The simulation focuses on operations in Feb 2025 as specified in the mission concept document but can also be applied on the backup date in September 2027 or any other date, when the asteroid is at a similiar distance to the sun. Due to the high eccentricity of the Alpha's heliocentric orbit, the solar radiation pressure will vary significantly over time. Consequently, if the arrival occurs near aphelion, the solar radiation pressure will be less than in the current scenario and the overall stability will be different.

Nevertheless, the orbits give good results for the current mission scenario. The small eccentricity of the stable orbits allow the generation of homogeneous remote sensing data set. Especially the laser altimeter will benefit from the almost constant altitudes. Additionally, the orbits are located in a sweet spot between the primary, secondaries and the solar radiation pressure and allow a precise gravity determination as no station keeping maneuvers will be required.
For carefully chosen initial states, in particular an initial eccentricity, frozen orbits exist in the model composed of sun, primary asteroid, S/C and Solar Radiation Pressure. This model does not account for the secondaries effect on s/c orbit. By analytical means we found initial conditions for frozen orbits. Numerical integration of frozen orbits are presented in section 4.2 and examples are visualized in Figure 5.
Terminator orbits at distances between 6 and 10 km were identified as suitable to conduct the second part of the ASTER science campaign. This orbit, named here simply as '8 km reference terminator orbit', is nearly circular and stays perpendicular to the incoming solar radiation at an average distance from Alpha's center of mass of about 8 km (presented in Figure 8).
The results also showed that a terminator orbit at a distance of approximately 2 km from the primary body Alpha ($<$ 1km from the surface) is possible (see Figure 7). However, this orbital region was not analyzed in detail as it would require a precise navigation through unstable areas were the effects of Gamma could cause critical instabilities. Additionally the specified stability zones between 6 and 10 km are an optimal choice to fulfil the science and laser requirements.
With the selected reference orbit at 8 km, laser ranging simulation could be performed. The results were used to analyze the exploration with the laser altimeter ALR under the described circumstances. In the case of a nadir pointing spacecraft, results point to a good coverage of low and high body latitude regions, with smaller concentration of measurement spots per area in central regions (white spots in Figure 10) and an increased one on the poles. However, depending on the primary's spin axis orientation (the uncertainty on this parameter is $\pm$15 deg), a small cap of uncovered area will probably remain over both, or at least one pole (the south one, in this simulation conditions). Because of that, to guarantee complete coverage of both poles, an important requirement for the attitude system of the s/c is the need to include an off-axis operation mode capability. This search has also pointed out that Terminator Orbits [26] are the most promising orbits for the achievement of the desired additional coverage of the poles of asteroid Alpha. Additionally, an observation of the primary and secondaries from a comparably close distance will also be possible.
This fact, combined with the very first investigation of a triple asteroid mission will allow collection of completely new scientific data and shed light on the evolution of Asteroids. This complementary exploration campaign of about 1-month with use of a terminator orbit and focused on the poles of asteroid Alpha is suggested to follow the first part of the main campaign which will use an encounter trajectory and focus on the central regions of Alpha.

Acknowledgements

The authors of this paper would like to thank two anonymous reviewers for their very helpful and constructive comments. Coauthor Antonio de Brum wishes to demonstrate his gratitude to the São Paulo Research Foundation - FAPESP, which supported his participation in this research (grant 2018/22672-4), also to the Planetary Research Institute of the German Aerospace Centre, in Berlin, where the research was conducted, and to the Federal University of ABC, in São Paulo, Brazil. Coauthor Friedrich Damme received funding by the Deutsche Forschungsgemeinschaft (DFG - German Research Foundation) for his research on sun-synchronous orbits. This research has made use of
- NASA's Astrophysics Data System
- data and/or services provided by the International Astronomical Union's Minor Planet Center and
- the scientific software shapeViewer (www.comet-toolbox.com).

References

[1] The International Astronomical Union IAU. Minor Planet Center. https://minorplanetcenter.net/, 2022. [Online; accessed 11-April-2022].

[2] Christian Gritzner, Kai Dürfeld, Jan Kasper, and Stefanos Fasoulas. The asteroid and comet impact hazard: risk assessment and mitigation options. *Naturwissenschaften*, 93(8):361–373, 2006.
[3] Clemens M. Rumpf, Hugh G. Lewis, and Peter M. Atkinson. Asteroid impact effects and their immediate hazards for human populations. *Geophysical Research Letters*, 44(8):3433–3440, 2017.
[4] J. L. Margot, M. C. Nolan, L. A. M. Benner, S. J. Ostro, R. F. Jurgens, J. D. Giorgini, M. A. Slade, and D. B. Campbell. Binary asteroids in the near-earth object population. *Science*, 296(5572):1445–1448, 2002.
[5] Julia Fang and Jean-Luc Margot. The Role of Kozai Cycles in Near-Earth Binary Asteroids. *The Astronomical Journal*, 143(3):59, 2012.
[6] Jean-Luc Margot, Petr Pravec, Patrick Taylor, Beno Carry, and Seth Jacobson. *Asteroid Systems Binaries, Triples, and Pairs*, pages 355–374. University of Arizona Press, 2015.
[7] David Parry Rubincam. Radiative Spin-up and Spin-down of Small Asteroids. *Icarus*, 148(1):2–11, 2000.
[8] Kevin J. Walsh, Derek C. Richardson, and Patrick Michel. Rotational breakup as the origin of small binary asteroids. *Nature*, 454:188, 2008.
[9] S. A. Jacobson and D. J. Scheeres. Evolution of Small Near-Earth Asteroid Binaries. In *EPSC-DPS Joint Meeting 2011*, volume 2011, page 647, October 2011.
[10] Matija Ćuk and Joseph A. Burns. Effects of thermal radiation on the dynamics of binary NEAs. *Icarus*, 176(2):418–431, August 2005.
[11] K. J. Walsh and S. A. Jacobson. *Formation and Evolution of Binary Asteroids*, pages 375–393. University of Arizona Press, 2015.
[12] Michael C. Nolan, E. S. Howell, T. M. Becker, C. Magri, J. D. Giorgini, and J. L. Margot. Arecibo Radar Observations of 2001 SN_{263}: A Near-Earth Triple Asteroid System. In *AAS/Division for Planetary Sciences Meeting Abstracts #40*, volume 40 of *AAS/Division for Planetary Sciences Meeting Abstracts*, page 25.04, September 2008.
[13] Marina Brozović, Lance A. M. Benner, Patrick A. Taylor, Michael C. Nolan, Ellen S. Howell, Christopher Magri, Daniel J. Scheeres, Jon D. Giorgini, Joseph T. Pollock, Petr Pravec, Adrián Galád, Julia Fang, Jean-Luc Margot, Michael W. Busch, Michael K. Shepard, Daniel E. Reichart, Kevin M. Ivarsen, Joshua B. Haislip, Aaron P. LaCluyze, Joseph Jao, Martin A. Slade, Kenneth J. Lawrence, and Michael D. Hicks. Radar and optical observations and physical modeling of triple near-Earth Asteroid (136617) 1994 CC. *Icarus*, 216(1):241–256, November 2011.
[14] Tracy M. Becker, Ellen S. Howell, Michael C. Nolan, Christopher Magri, Petr Pravec, Patrick A. Taylor, Julian Oey, David Higgins, Jozef Vilagi, Leonard Kornos, Adrian Galad, Stefan Gajdos, Ninel M. Gaftonyuk, Yurij N. Krugly, Igor E. Molotov, Michael D. Hicks, Albino Carbognani, Brian D. Warner, Frederic Vachier, Franck Marchis, and Joseph T. Pollock. Physical modeling of triple near-earth asteroid (153591) 2001 sn263 from radar and optical light curve observations. *Icarus*, 248:499–515, 2015.
[15] Tracy Michelle Becker, M. Nolan, E. Howell, and C. Magri. Physical Modeling of Triple Near-Earth Asteroid 153591 (2001 SN263). In *American Astronomical Society Meeting Abstracts #213*, volume 213 of *American Astronomical Society Meeting Abstracts*, page 401.10, January 2009.
[16] T. M. Becker, E. S. Howell, M. C. Nolan, C. Magri, P. Pravec, P. A. Taylor, J. Oey, D. Higgins, J. Vilagi, L. Kornos, A. Galad, S. Gajdos, N. M. Gaftonyuk, Yu. N. Krugly, I. E. Molotov, M. D. Hicks, A. Carbognani, B. D. Warner, F. Vachier, F. Marchis, and J. T. Pollock. Shape model of Asteroid (153591) 2001 SN263 V1.0. *NASA Planetary Data System*, October 2017.
[17] A. A. Sukhanov, H. F. C. Velho, E. E. N. Macau, and O. C. Winter. The Aster project: Flight to a near-Earth asteroid. *Cosmic Research*, 48(5):443–450, 2010.
[18] E. E. N. Macau, O. C. Winter, H. F. C. Velho, A. A. Sukhanov, A. G. V. Brum, J. L. Ferreira, A. Hetem, and G. M. Sandonato. The ASTER mission: exploring for the first time a triple system asteroid. In *Proceedings of the 62nd International Astronautical Congress*, Cape Town, SA, 2011.
[19] A. G. V. Brum, H. Hussmann, K. Wickhusen, and A. Stark. Encounter trajectories for Deep Space Mission ASTER to the triple Near Earth Asteroid 2001-SN263. The laser altimeter (ALR) point of view. *Advances in Space Research*, 2021.
[20] Yuichi Tsuda, Makoto Yoshikawa, Masanao Abe, Hiroyuki Minamino, and Satoru Nakazawa. System design of the Hayabusa 2 Asteroid sample return mission to 1999 JU3. *Acta Astronautica*, 91:356–362, October 2013.
[21] Hajime Yano, T. Kubota, H. Miyamoto, T. Okada, D. Scheeres, Y. Takagi, K. Yoshida, M. Abe, S. Abe, O. Barnouin-Jha, A. Fujiwara, S. Hasegawa, T. Hashimoto, M. Ishiguro, M. Kato, J. Kawaguchi, T. Mukai, J. Saito, S. Sasaki, and M. Yoshikawa. Touchdown of the Hayabusa Spacecraft at the Muses Sea on Itokawa. *Science*, 312(5778):1350–1353, June 2006.
[22] D. S. Lauretta, S. S. Balram-Knutson, E. Beshore, W. V. Boynton, C. Drouet d'Aubigny, D. N. DellaGiustina, H. L. Enos, D. R. Golish, C. W. Hergenrother, E. S. Howell, C. A. Bennett, E. T. Morton, M. C. Nolan, B. Rizk, H. L. Roper, A. E. Bartels, B. J. Bos, J. P. Dworkin, D. E. Highsmith, D. A. Lorenz, L. F. Lim, R. Mink, M. C. Moreau, J. A. Nuth, D. C. Reuter, A. A. Simon, E. B. Bierhaus, B. H. Bryan, R. Ballouz, O. S. Barnouin, R. P. Binzel, W. F. Bottke, V. E. Hamilton, K. J. Walsh, S. R. Chesley, P. R. Christensen, B. E. Clark, H. C. Connolly, M. K. Crombie, M. G. Daly, J. P. Emery, T. J. McCoy, J. W. McMahon, D. J. Scheeres, S. Messenger, K. Nakamura-Messenger, K. Righter, and S. A. Sandford. OSIRIS-REx: Sample Return from Asteroid (101955) Bennu. *Space Science Reviews*, 212(1-2):925–984, October 2017.
[23] Andrew F. Cheng, Andrew S. Rivkin, Patrick Michel, Justin Atchison, Olivier Barnouin, Lance Benner, Nancy L. Chabot, Carolyn Ernst, Eugene G. Fahnestock, Michael Kueppers, Petr Pravec, Emma Rainey, Derek C. Richardson, Angela M. Stickle, and Cristina Thomas. AIDA DART asteroid deflection test: Planetary defense and science objectives. *Planetary and Space Science*, 157:104–115, August 2018.
[24] Colin R. McInnes. The Existence and Stability of Families of Displacement Two-Body Orbits. *Celestial Mechanics and Dynamical Astronomy*, 67(2):167–180, February 1997.

[25] D. J. Scheeres. Satellite dynamics about small bodies: Averaged solar radiation pressure effects. *Journal of the Astronautical Sciences*, 47(1):25–46, 1999.
[26] H. Hussmann, J. Oberst, X. Wickhusen, K.and Shi, F. Damme, F. Lüdicke, V. Lupovka, and S. Bauer. Stability and evolution of orbits around the binary asteroid 175706 (1996 fg3): Implications for the marcopolo-r mission. *Planetary and Space Science*, 70(1):102–113, 2012.
[27] J. Bookless and C. McInnes. Dynamics and control of displaced periodic orbits using solar-sail propulsion. *J. Guid. Control Dyn.*, 29(3):527–537, 2006.
[28] Marco Giancotti, Stefano Campagnola, Yuichi Tsuda, and Jun'ichiro Kawaguchi. Families of periodic orbits in Hill's problem with solar radiation pressure: application to Hayabusa 2. *Celestial Mechanics and Dynamical Astronomy*, 120(3):269–286, November 2014.
[29] D. Scheeres, B.M. Sutter, and Aaron Rosengren. Design, dynamics and stability of the osiris-rex sun-terminator orbits. *Advances in the Astronautical Sciences*, 148:3263–3282, 01 2013.
[30] Siamak G. Hesar, Daniel J. Scheeres, and Jay W. McMahon. Sensitivity Analysis of the OSIRIS-REx Terminator Orbits to Maneuver Errors. *Journal of Guidance Control Dynamics*, 40(1):81–95, January 2017.
[31] Antonio F. B. A. Prado. Mapping orbits around the asteroid 2001sn263. *Advances in Space Research*, 53(5):877–889, 2014.
[32] R. A. N. Araujo, O. C. Winter, A. F. B. A. Prado, and A. A. Sukhanov. Stability regions around the components of the triple system 2001 sn263. *Monthly Notices of the Royal Astronomical Society*, 423(4):3058–3073, 2012.
[33] R. A. N. Araujo, O. C. Winter, and A. F. B. A. Prado. Stable retrograde orbits around the triple system 2001 sn263. *Monthly Notices of the Royal Astronomical Society*, 449(4):4404–4414, 2015.
[34] B. Y. P. L. Masago, A. F. B. A. Prado, A. P. M. Chiaradia, and V. M. Gomes. Developing the precessing inclined bi-elliptical four-body problem with radiation pressure to search for orbits in the triple asteroid 2001sn263. *Advances in Space Research*, 57(4):962–982, 2016.
[35] J. B. Silva Neto, D. M. Sanchez, A. F. B. A. Prado, J. K. S. Formiga, R. Zanetti, R. P. Russell, M. T. Ozimek, and A. L. Bowes. Using solar radiation pressure to maneuver a spacecraft in the triple asteroid 2001sn(263). *Spaceflight Mechanics*, 158:3789–3804, 2016.
[36] Marina Cavalca, Antonio F. B. A. Prado, Jorge Formiga, and V. Gomes. Searching for orbits around the triple asteroid 2001sn 263. *Journal of Physics: Conference Series*, 9111:012008, 2017.
[37] D. M. Sanchez and A. F. B. A. Prado. Searching for less-disturbed orbital regions around the near-earth asteroid 2001 sn263. *Journal of Spacecraft and Rockets*, 56(6):1775–1785, 2019.
[38] Guillaume Obrecht, Kevin Cowan, and Antonio Fernand de Almeida Prado. Applicability of evolutionary algorithms for orbit optimization in the strongly perturbed environment of the 2001 SN263 triple asteroid system. *Proceedings of the 2nd IAA/AAS SciTech Forum 2019 (SciTech Forum on Space Flight Mechanics and Space Structures and Materials), Moscow, Russia, 25 June 2019*, 174:205–225, 2020.
[39] D. Perna, A. Alvarez-Candal, S. Fornasier, Z. Kaňuchová, S. M. Giuliatti Winter, E. Vieira Neto, and O. C. Winter. The triple near-Earth asteroid (153591) 2001 SN263: an ultra-blue, primitive target for the Aster space mission. *Astronomy and Astrophysics*, 568:L6, August 2014.
[40] V. Goretov, A. Lipatov, and V. Linkin. Description of the spacecraft on the EJP for near-earth and planetary research. Technical Report IKI-ASTER-DS-01, Space Research Institute of the Russian Academy of Sciences, March 2018.
[41] A. G. V. Brum, A. Hetem Jr, I. S. Rego, C. P. F. Francisco, A. Fenili, F. Madeira, F. C. Cruz, and M. Assafin. Preliminary development plan of the ALR, the laser rangefinder for the ASTER deep space mission to the 2001 SN263 asteroid. *Journal of Aerospace Tech and Management*, 3(3):331–338, 2011.
[42] A. G. V. Brum and F. C. Cruz. Reviewed plan of the ALR, the laser rangefinder for the ASTER deep space mission to the triple asteroid 2001-SN263. *Journal of Physics: Conf. Ser.*, 911(012016), 2017.
[43] A. G. V. Brum, A. Hetem Jr, and F. C. Cruz. ALR – Laser altimeter for the ASTER deep space mission. Simulated operation above a surface with crater. *Journal of Physics: Conf. Ser.*, 641(012007), 2015.
[44] A. G. V. Brum, A. Hetem Jr, F. C. Cruz, and A. P. Rodrigues. ALR - A laser altimeter for the first Brazilian deep space mission. Modeling and simulation of the instrument and its operation. *Journal of Computational and Applied Mathematics*, 34(2):557–569, 2015.
[45] O. C. Winter, G. Valvano, T. S. Moura, G. Borderes-Motta, A. Amarante, and R. Sfair. Asteroid triple-system 2001 SN263: surface characteristics and dynamical environment. *Monthly Notices of the Royal Astronomical Society*, 492(3):4437–4455, 2020.
[46] O. Montenbruck and E. Gill. *Satellite orbits : models, methods, and applications*. Springer Science, January 2000.
[47] A. F. Cheng, O. S. Barnouin, C. M. Ernst, and E. G. Kahn. Efficient Calculation of Effective Potential and Gravity on Small Bodies. In *Asteroids, Comets, Meteors 2012*, volume 1667 of *LPI Contributions*, page 6447, May 2012.
[48] R. A. Werner and D. J. Scheeres. Exterior gravitation of a polyhedron derived and compared with harmonic and mascon gravitation representations of asteroid 4769 Castalia. *Celestial Mechanics and Dynamical Astronomy*, 65:313–344, September 1996.
[49] Mark A. Wieczorek and Matthias Meschede. Shtools: Tools for working with spherical harmonics. *Geochemistry, Geophysics, Geosystems*, 19(8):2574–2592, 2018.
[50] T. Mizuno, T. Kase, T. Shiina, M. Mita, N. Namiki, H. Senshu, R. Yamada, H. Noda, H. Kunimori, N. Hirata, F. Terui, and Y. Mimasu. Development of the laser altimeter (lidar) for hayabusa2. *Space Science Reviews*, 208(1):33–47, 2017.
[51] S. Takahashi and D. J. Scheeres. Higher-Order Corrections for Frozen Terminator Orbit Design. *Journal of guidance, control and dynamics*, 43(9):1642–1655, 2020.
[52] S. B. Broschart, D. J. Scheeres, and B. F. Villac. New families of multi-revolution terminator orbits near small bodies.